

Edward MURDZIA*, Stanisław STRZELECKI**

CALCULATIONS OF TILTING-PAD THRUST BEARINGS

OBLICZENIA ŁOŻYSK ŚLIZGOWYCH WZDŁUŻNYCH Z SEGMENTAMI WAHLIWYMI

Key words: hydrodynamic lubrication, thrust bearings, static characteristics.

Abstract: The application of thrust bearings in different engineering designs generates problems of thermal state, which generates the wear of the fixed or tilting pads of bearings. These problems can be avoided by means of proper methods and numerical algorithms of calculations of the bearing static characteristics, including the maximum oil film temperature. The knowledge of thermal state of bearings should assure safe, reliable, and durable bearing operation and is important for the designers of thrust bearings. This paper presents the results of calculations of some static characteristics of a tilting-pad thrust bearing, including its maximum oil film temperature. Numerical solution by means of finite differences was applied for the solution of geometry, Reynolds, energy, and viscosity equations. Adiabatic oil film laminar flow in the bearing gap was considered. The developed code of the computation of bearing performances creates a tool that leads to the solution of thermal problems. Different values of operating speeds were assumed.

Słowa kluczowe: smarowanie hydrodynamiczne, łożyska wzdluzne, charakterystyki statyczne.

Streszczenie: Stosowanie ślizgowych łożysk wzdluznych wiąże się z problemami stanu cieplnego i zużycia stałych lub wahlwiyh segmentów łożyska. Zastosowanie odpowiednich metod obliczeniowych i algorytmów numerycznych charakterystyk statycznych łożyska włącznie z maksymalną temperaturą filmu smarowego pozwala na uniknięcie problemów eksploatacyjnych. Znajomość stanu cieplnego łożyska powinna zapewnić bezpieczną, niezawodną, trwałą jego eksploatację oraz jest ważna dla konstruktorów łożysk wzdluznych. W artykule przedstawiono wyniki obliczeń niektórych charakterystyk statycznych łożyska wzdluznego z segmentami wahlwiyh. Podstawowe równania teorii smarowania hydrodynamicznego Reynoldsa, energii i lepkości oraz geometrii rozwiązano metodą iteracyjną. Opracowany algorytm obliczeń numerycznych łożyska z nieizotermicznym filmem smarowym stwarza narzędzie pozwalające na rozwiązywanie problemów cieplnych łożysk wzdluznych. Założono różne wartości prędkości obrotowych. Przyjęto adyabatyczny, laminarny model filmu smarowego.

INTRODUCTION

Thrust bearings are widely applied in different engineering applications like mechanical seals, machine tool ways, piston rings, plain collar thrust bearings, cryogenic high speed turbo-machinery, etc. Thermal, turbulence and inertial effects will affect lubricant flow in the bearings [L. 1–6]. The temperatures of pad surfaces and lubricant increase with the increase in slider speed resulting in a very narrow safety margin against seizure.

One of the most important limitations that do not allow for any increase in loads and rotational speeds of thrust bearings is the temperature of the lubricant. The temperature increase of the lubricating oil is caused by the amount of heat released in the oil film during the operation of the bearing. Sliding thrust bearings with large overall dimensions and tilting pads are used in the bearing system of the main shafts of marine steam turbines and water turbines, spindles of heavy machine tools, gears, etc. In this case, while transmitting significant power, the

* Łódź, Poland.

** ORCID: 0000-0001-5030-5249. Łódź, Poland.

power losses due to friction also reach high values. The cooling of the tilting pads in the thrust bearing of a generator driven by a water turbine [L. 3] allowed for the reduction of the operating surface of the bearing by half while reducing friction losses from 42 kW to 25 kW. Thermal phenomena occurring in the oil film have to be considered in the process of designing and calculating a bearing.

In order to take advantage of the possibilities of heat release from the oil film and hydrostatic lifting, a design solution (Fig. 1) was proposed for the use of lubricating oil as a cooling medium of the bearing pad [L. 3].

Another problem that is important from the technical point of view is the transition from mixed friction to fluid friction and vice versa in the start-up and stopping phase of bearing assembly. Shortening the time of this transition has a significant impact on reducing the wear of the friction surfaces, as well as reducing the amount of heat generated at the same time. In practice, this problem is solved by hydrostatic lifting, the so-called "leverage" of the shaft, which requires the use of a high-pressure feed oil installation. This has the effect of a lifting pocket on THD performance of a large tilting-pad thrust bearing in the power plant [L. 4, 8, 13]. The results show that hydrostatic recess changes calculated bearing properties, particularly in vicinity of the pocket.

The phenomena of the inlet temperature of supplied oil are complex and, in many cases, further affected by any special arrangements of pressurized oil supply to the gap between pads. The reason for such arrangements is the more efficient supply of externally cooled lubricant. Preliminary results of modelling lubricant flow in the gap in a bearing with direct oil supply system are presented in this paper [L. 14].

In [L. 10], the pad temperatures profile-sliding surface, oil pressure in hydrodynamic gap, and film geometry are compared to the measured values. The results given in [L. 15] confirmed that the load-carrying capacity of the flat land bearing is poor, and the additional hydrostatic lubrication improves its performance. The speed is found to be a critical parameter; as it increases, the hydrostatic effect is affected and the film thickness is reduced.

The problems of axial thrust tilting-pad bearings are very complex and their solution requires a proper method of calculations combined with robust computer programs. The phenomenon of the heat dissipated from the lubricating film

through the elements limiting it to the environment and the influence of on the operating characteristics of the bearing is still controversial. It requires more works on the operation and static characteristics of considered bearings.

This paper presents the results of the numerical calculation of chosen static characteristics of tilting-pad thrust bearing. Different models of oil film were assumed, i.e. isothermal, adiabatic, and diathermic. The solution of the basic equations of thermo-hydrodynamic theory of lubrication gives the necessary data on the pressure, temperature distributions, the maximum value of pressure, the temperature of oil film, the minimum oil film thickness, oil flow, and friction forces, that determine the static characteristics determining the input variables for the design of bearing. Theoretical results were compared to the experimental obtained on the test rig.

GEOMETRY OF THE OIL FILM

It is assumed that the oil film is restricted on one side by a bearing pad and on the other by a thrust plate. The edge of the oil film is defined by the pad profile [L. 1–3, 7].

It was assumed that the bearing pad is a segment of a circular ring (Fig. 1); therefore, the geometries of the oil film are restricted by the following boundaries:

$$R_1 \leq r \leq R_2 \quad 0 \leq \varphi \leq \delta \quad 0 \leq z \leq h \quad (1)$$

where: h – oil film thickness (μm), R_1 , R_2 – inner and outer radius (m), r , φ , z – coordinates of a cylindrical system, δ – angle of pad (rad).

The thickness of the oil film can be represented by the following relationship [L. 3, 7]:

$$h = h_n + \Sigma h_m + h_o \quad (2)$$

where: h_n – nominal oil film thickness measured between undistorted surfaces adjacent to the side surfaces of the mating elements bearings, h_m – oil film thickness measured between the surface adjacent to the surface and the actual, (rough) surface of the sliding elements, h_o – oil film thickness change due to thermoelastic deformation the sliding elements of the bearing.

The research carried in [L. 1] shows that, for a small roughness, often used in practice, their influence on the operating characteristics of the bearing is negligible; therefore, this component was omitted in the presented work, i.e. it was assumed that $\sum h_m = 0$.

The theoretical and experimental studies in [L. 2] show that, for the ratio of the pad thickness to its width – of the order $H/B = 0.2$ (and thus the most commonly used in practice), the deformations occurring are small and have a negligible influence on the bearing characteristics.

Therefore, the component which takes into account deformations is neglected, i.e. $h_o = 0$.

The nominal thickness of the lubricating film was determined assuming that the surfaces adjacent to the pad and the thrust washer are planes.

It has been assumed that the lubricating gap is formed as a result of establishing the average thickness of the lubricating film h_s , and, as a result of the rotation of the tilting-pad around two mutually perpendicular axes S_x and S_y intersecting

at the point with coordinates $S(R_s, \delta_0, h_s)$, this point corresponds to the support point of the pad.

Hence, the relationship on the nominal thickness of the lubricating film at any point was derived in the following form:

$$h_n = h_s + m_1 x + m_2 y_0 \tag{3}$$

where: m_1, m_2 – tangents of rotation angle of pad around the axis s_y and s_x .

Neglecting, in Equation (2), the terms of roughness and deformations and applying the cylindrical coordinates system r, φ, z the dependence on the lubricating film thickness has the following form:

$$h = h_s - r \sin(\delta_0 - \varphi) m_1 + [r \cos(\delta_0 - \varphi) - R_s] m_2 \tag{4}$$

where: h_s – oil film thickness at the point S, δ_0 – angle of pad support.

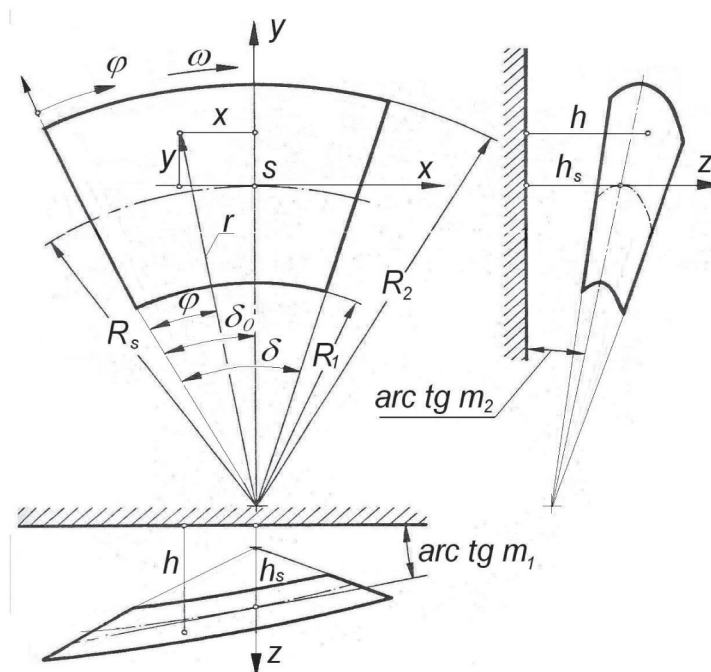


Fig. 1. Oil film geometry

Rys. 1. Geometria filmu smarowego

DIMENSIONLESS FORM OF BASIC EQUATIONS

The dimensionless equations describing the oil film pressure, temperature distributions, and the characteristics of bearing [L. 1–3, 7] have the form given below.

Equation of oil film pressure distribution:

$$\frac{\partial^2 \bar{p}}{\partial \bar{r}^2} + \left(\frac{3}{\bar{h}} \frac{\partial \bar{h}}{\partial \bar{r}} + \frac{1}{\bar{r}} - \frac{1}{\eta} \frac{\partial \bar{\eta}}{\partial \bar{r}} \right) \frac{\partial \bar{p}}{\partial \bar{r}} + \left(\frac{3}{\bar{h}} \frac{\partial \bar{h}}{\partial \bar{\varphi}} - \frac{1}{\eta} \frac{\partial \bar{\eta}}{\partial \bar{\varphi}} \right) \frac{1}{\delta^2 \bar{r}^2} + \frac{1}{\bar{r}^2 \delta^2} \frac{\partial^2 \bar{p}}{\partial \bar{\varphi}^2} - 6 \frac{\bar{\eta}}{\delta \bar{h}^3} \frac{\partial \bar{h}}{\partial \bar{\varphi}} = 0 \quad (5)$$

where: \bar{h} – dimensionless oil film thickness $\bar{h} = h/h_s$, \bar{p} – dimensionless oil film pressure, $\bar{p} = p h_s / \eta_0 \omega R_s^4$, p – oil film pressure (MPa), R_s – mean radius of the plate, ω – angular velocity (sec^{-1}), \bar{r} , $\bar{\varphi}$ – dimensionless radial and peripheral co-ordinates, η – dimensionless viscosity of lubricant $\eta = \eta/\eta_0$, η_0 – dynamic oil viscosity at the reference temperature Ns/m^2 .

Energy equation:

$$P_e K_T (\bar{q}_r \frac{\partial \bar{T}}{\partial \bar{r}} + q_\varphi \frac{1}{\delta \bar{r}} \frac{\partial \bar{T}}{\partial \bar{\varphi}}) = -\bar{k}_1 (\bar{T} - T_c) + \Lambda K_T \frac{\bar{h}^3}{12 \eta} \cdot \left[\left(\frac{\partial \bar{p}}{\partial \bar{r}} \right)^2 + \frac{1}{\delta^2} \left(\frac{\partial \bar{p}}{\bar{r} \partial \bar{\varphi}} \right)^2 \right] + \Lambda K_T \frac{\bar{r}^2 \bar{\eta}}{\bar{h}} \quad (6)$$

where: \bar{T} – dimensionless oil film temperature, $\bar{T} = T/T_0$, P_e – Peclet number, $P_e = \rho c \omega r^2 / \lambda$, ρ : oil density, T_c – average temperature of oil film K , K_r – thermal coefficient, $K_T = \omega \cdot \eta_0 / c_i \cdot \rho \cdot g \cdot T_0 \cdot \omega^2$, (kg/m^3), c_i – oil specific heat, (J/kgK), λ – heat transfer coefficient ($\text{W/m}^2\text{K}$), \bar{q}_r – oil flow in radial and peripheral directions $\bar{q}_r = -\frac{\bar{h}^3}{12 \eta} \frac{\partial \bar{p}}{\partial \bar{r}}$, $\bar{q}_\varphi = -\frac{\bar{h}^3}{12 \eta} \frac{\partial \bar{p}}{\partial \bar{\varphi}} + \frac{\bar{h} \bar{r}}{2}$.

Oil viscosity is described by the following exponential equation [L. 1, 2]:

$$\bar{\eta} = e^{A(\bar{T} - \bar{T}_0) + B(\bar{T} - \bar{T}_0)^2} \quad (7)$$

where: A, B – dimensionless viscosity-temperature coefficients [L. 3] determined experimentally for considered lubricant.

Oil film thickness (gap geometry):

$$\bar{h} = 1 - \frac{m_1 R_s}{h_s} \bar{r} \sin(\bar{\delta}_0 - \bar{\varphi}) + \frac{m_2 R_s}{h_s} [\bar{r} \cos \delta (\delta_0 - \bar{\varphi}) - 1] \quad (8)$$

where: $\bar{\delta}_0$ – dimensionless angle of pad support.

The following boundary conditions of pressure field are assumed:

$$\bar{p}(\bar{R}_1, \varphi, \bar{z}) = \bar{p}(\bar{R}_2, \varphi, \bar{z}) = \bar{p}(\bar{r}, 1, \bar{z}) = 0 \quad (9)$$

For the temperature field the boundary conditions given below are given:

$$\bar{T}(\bar{r}, 0, \bar{z}) = 1$$

$$\bar{T}(\bar{r}) \Big|_{\bar{r}=\bar{R}_1}^{\bar{r}=\bar{R}_1+\Delta r} = A_1 + B_1 r + C_1 \bar{r}^2 \quad (10)$$

$$\bar{T}_c = 1 - \Delta \bar{T} / 2$$

where: A_1, B_1, C_1 – constants.

Thrust bearing static characteristics expressed by the load capacity \bar{W} , polar coordinates of resultant force \bar{r}_w and $\bar{\varphi}_w$, friction torque \bar{M}_t , oil flow at inlet and outlet \bar{Q}_{wl} , \bar{Q}_{wyl} and side oil flow \bar{Q}_b give the equations (1) through (7) respectively.

$$\bar{W} = \int_{\bar{R}_1}^{\bar{R}_2} \int_0^1 \bar{p} \bar{r} d\bar{r} d\bar{\varphi} \quad (11)$$

$$\bar{r}_w = \sqrt{\bar{x}_w^2 + \bar{y}_w^2} \quad (12)$$

$$\bar{\varphi}_w = \frac{1}{\delta} \arctg \frac{\bar{y}_w}{\bar{x}_w} \quad (13)$$

$$\bar{M}_t = - \int_{\bar{R}_1}^{\bar{R}_2} \int_0^1 \left(\frac{\bar{r} \bar{h}}{2} \frac{\partial \bar{p}}{\partial \bar{\varphi}} + \frac{\bar{r}^3 \bar{\eta} \delta}{\bar{h}} \right) d\bar{r} d\bar{\varphi} \quad (14)$$

$$\bar{Q}_{wl} = \int_{\bar{R}_1}^{\bar{R}_2} \bar{q}_\varphi \Big|_{\bar{\varphi}=0} d\bar{r} \quad (15)$$

$$\bar{Q}_{wyf} = \int_{\bar{R}_1}^{\bar{R}_2} \bar{q}_\varphi |_{\bar{\varphi}=1} d\bar{r} \quad (16)$$

$$\bar{Q}_b = \bar{Q}_{wl} - \bar{Q}_{wyf} \quad (17)$$

The system of equations (5) through (17) was solved by means of the finite difference method [L. 29, 30] with the use of appropriate number of mesh points [L. 1–3].

The points of coordinates $(\bar{r}_i, \bar{\varphi}_j)$ correspond the mesh points:

$$\begin{aligned} \bar{r}_i &= \bar{R}_1 - (i-1)\Delta\bar{r} \quad i = 1, 2, \dots, l \\ \bar{\varphi}_j &= (j-1)\Delta\bar{\varphi} \quad j = 1, 2, \dots, m \end{aligned} \quad (18)$$

where: i, j – mesh points in radial and peripheral direction, l, m – number of assumed point of mesh.

Mesh scale in the radial and peripheral direction is as follows, respectively:

$$\begin{aligned} \Delta\bar{r} &= \frac{\bar{R}_2 - \bar{R}_1}{l-1} \\ \Delta\bar{\varphi} &= \frac{1}{m-1} \end{aligned} \quad (19)$$

After some tests, it was assumed that the mesh with the number of nodes $l \times m = 11 \times 21$ assures good results.

Exemplary, for the mesh 15x21, the difference in the determination of maximum oil film pressure is not larger than 0.01% with the respect to the pressure which was determined at application of mesh 11x21 points, but for the temperature, this difference does not overcome 0.0003%.

For the finding the discrete values of the functions in the single point of mesh, the equations (3) and (4) were transformed to the difference form [L. 3]. In the equations of pressure and temperature the partial derivatives were replaced by differential (central) quotients.

The derivatives of oil film thickness $\partial\bar{h}/\partial\bar{r}$ and $\partial\bar{h}/\partial\bar{\varphi}$ were found analytically [L. 2, 3].

The developed algorithm allows the calculations of oil film pressure and temperature distribution, velocities, and characteristics of the bearing, such as the following: load capacity, friction torque, and the coordinates of point of load capacity vector and oil streams.

The input parameters for the code of numerical calculations were the oil film thickness in the point with the coordinated (R_s, δ_0) , the physical properties of lubricant, and the angular speed of thrust disc.

RESULTS OF CALCULATIONS

Preliminary results that were obtained from developed code of numerical computations of tilting-pad thrust bearing static characteristics comprise the following: oil film pressure and temperature distributions and their maximum values, load capacity, and friction torque.

The following geometrical and operational data were assumed: oil film thickness h_s at the point with coordinates (R_s, δ_0) , inner and outer radii of the plate R_1 and R_2 , tangents of rotation angle of the pad around the axis s_y and s_x m_1 and m_2 , δ, δ_0 – angle of pad, and the angle of supported line, respectively, dynamic oil viscosity coefficient η , dynamic oil viscosity coefficient at the reference temperature η_0 , thermal conductivity coefficient in the oil λ , thermal conductivity coefficient in the pad η_p , factors taking into account the effect of temperature on the oil viscosity a, b , average temperature of oil film T_c , reference temperature T_0 , temperature of oil at inlet edge T_p , and heat transfer coefficient k_t .

The range of rotational speeds was varied from 50 rpm through 1000 rpm.

Exemplary results of computations are presented in Fig. 2 through Fig. 11.

Figure 2 through Fig. 5 present the oil film pressure distributions – Fig. 2 three dimensional, Fig. 3 in peripheral direction, Fig. 4 in radial direction and Fig. 5 isobars of pressure (for rotational speed $n = 100$ rpm). Oil film thickness distribution is shown in Fig. 6.

Maximum values of pressure p_{\max} and temperature T_{\max} with the responding point of their position that are showed in Fig. 2 are as follows: $p_{\max} = 2.6$ MPa at $i = 7$ and $j = 17$, in case of $T_{\max} = 55.41^\circ\text{C}$, $i = 11$ and $j = 21$. Figure 3 shows the oil film pressure distribution on the pad length (peripheral direction); it can be seen that the $p_{\max} = 0.07$ MPa at the coordinates $i = 16$ and $j = 5$.

An example of oil film distribution in the radial direction on the pad is shown in Fig. 4. The isobars of pressure in oil film are shown in Fig. 5. Oil film temperature 3-dimensional distribution for adiabatic model of oil film is shown in Fig. 7, along with the maximum value of temperature T_{\max} . The

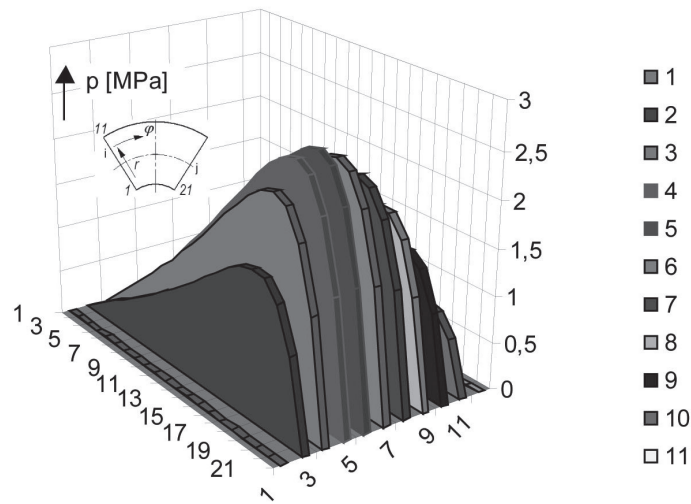


Fig. 2. 3-D distribution of oil film pressure

Rys. 2. 3-D rozkład ciśnienia w filmie smarowym

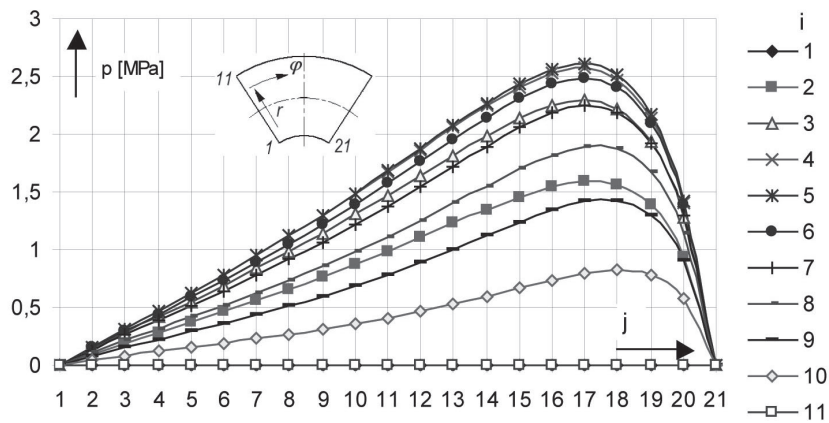


Fig. 3. Oil film pressure distribution on the pad length (peripheral direction)

Rys. 3. Rozkład ciśnienia w filmie smarowym na długości segmentu (kierunek obwodowy)

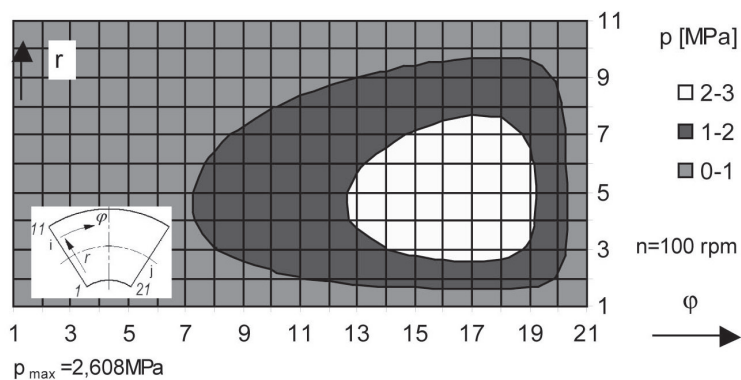


Fig. 4. Isobars of oil film pressure

Rys. 4. Izobary rozkładu ciśnienia w filmie smarowym

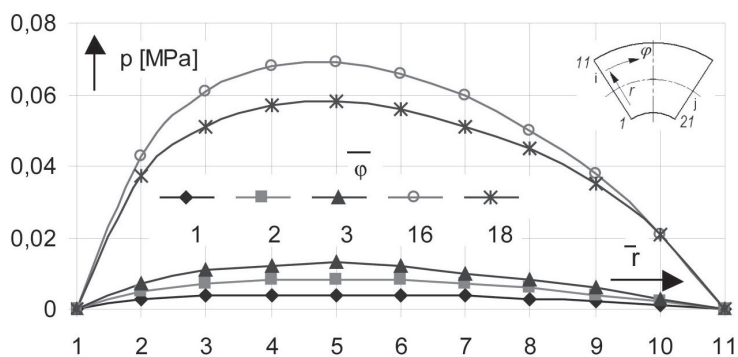


Fig. 5. Oil film pressure distribution on the pad width (radial direction)

Rys. 5. Rozkład ciśnienia na szerokości segmentu (kierunek promieniowy)

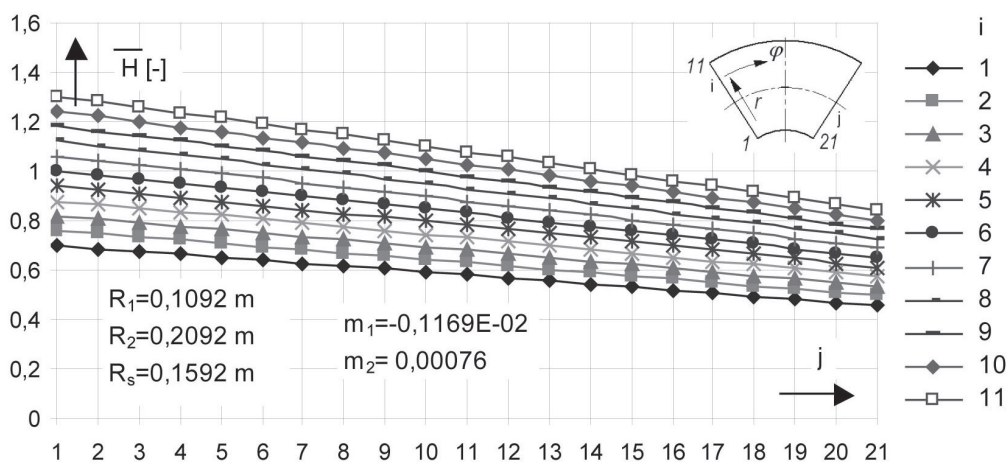


Fig. 6. Oil film thickness distribution

Rys. 6. Rozkład grubości filmu smarowego

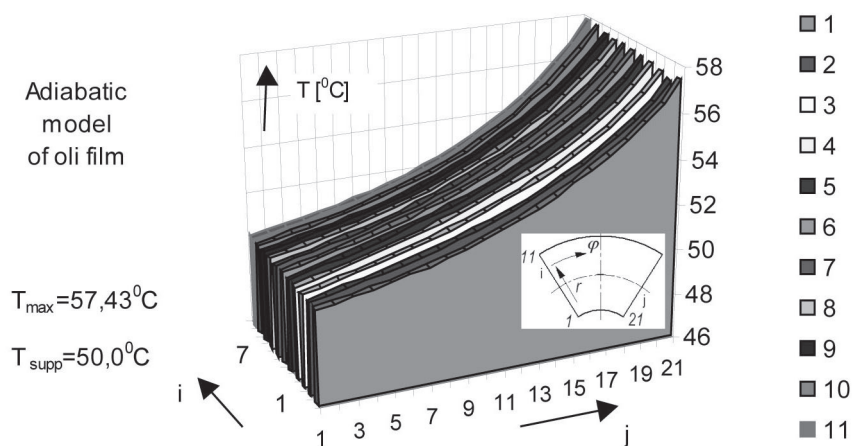


Fig. 7. 3-D distribution of oil film temperature

Rys. 7. 3-D rozkład temperatury

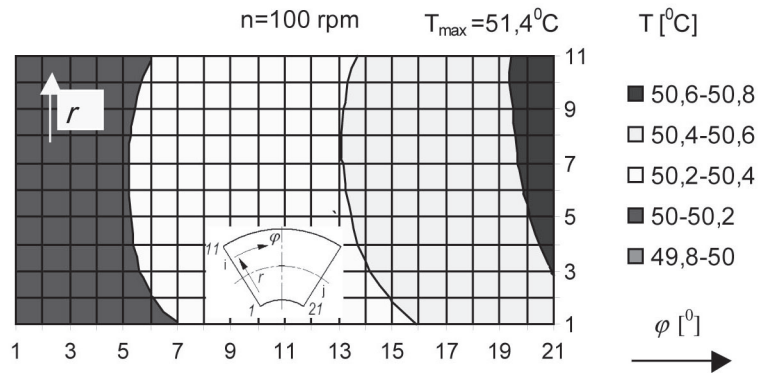


Fig. 8. Isotherms of oil film temperature
 Rys. 8. Izotermi rozkładu temperatury

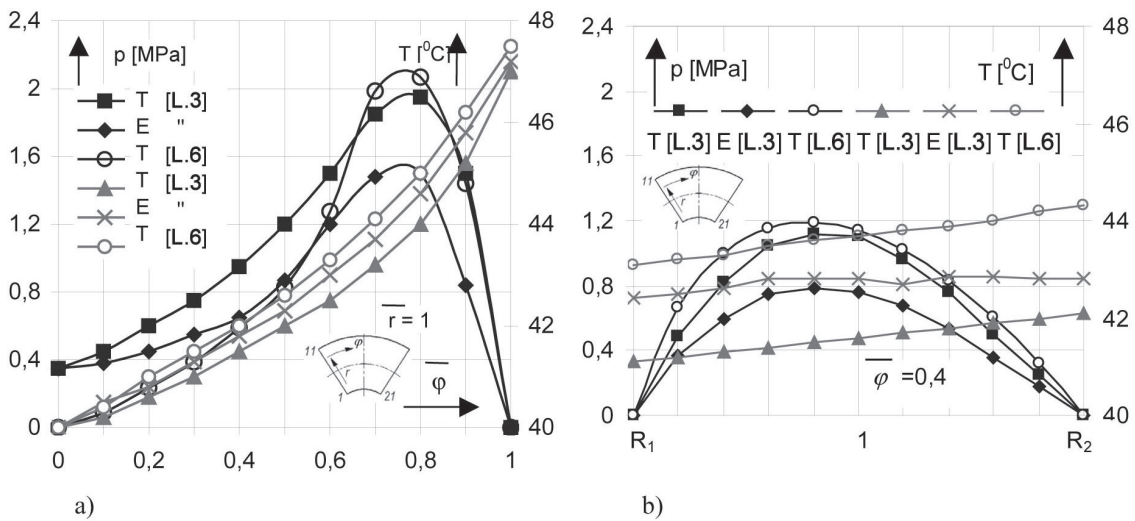


Fig. 9. Comparison of oil film pressure and temperature distributions; T – theory, E – experiment
 Rys. 9. Porównanie rozkładów ciśnienia i temperatury w filmie olejowym; T – teoria, E – doświadczenie

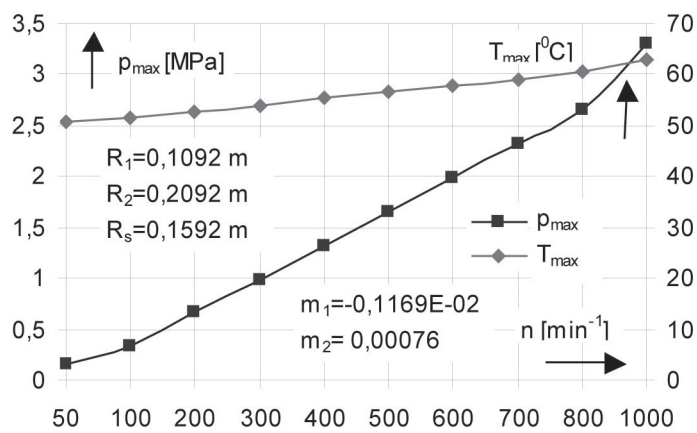


Fig. 10. Load capacity and friction torque at different rotational speeds of the disc of axial thrust bearing
 Rys. 10. Nośność i moment tarcia dla różnych prędkości obrotowych tarczy łożyska wzdłużnego

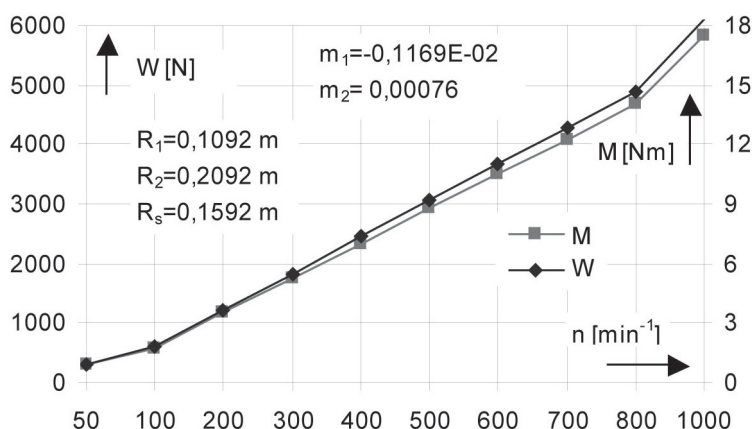


Fig. 11. Maximum oil film pressure and temperature at different rotational speeds of the disc of axial thrust bearing
 Rys. 11. Maksymalne wartości ciśnienia i temperatury dla różnych prędkości obrotowych tarczy łożyska wzdłużnego

isotherms of oil film temperature distribution can be observed in **Fig. 8**.

Figure 9 shows the comparison of the oil film pressure and temperature distributions obtained theoretically and experimentally [**L. 3, 6**] in the peripheral (**Fig. 9a**) and radial (**Fig. 9b**) directions. The maximum values of pressure that were obtained in [**L. 6**] are close to the values obtained in [**L. 3**]; the differences can be explained by the assumed data and pressurized lubricant supply (see $\bar{\varphi} = 0$, **Fig. 9a**).

The load capacity W and friction torque M are shown in **Fig. 10**. Maximum values of pressure p_{\max} and temperature T_{\max} for assumed range of rotational speeds are shown in **Fig. 11**.

FINAL REMARKS

Theoretical considerations and experimental studies carried out, as well as the analysis of the results, allow for the formulation of the following conclusions:

1. The theoretical model of a bearing well reflects the physical phenomena occurring in a real thrust bearing operating at different sliding speeds.
2. The developed code of the numerical calculation of static characteristics of the thrust tilting-pad bearing gives the results that are comparable to the experimental ones.
3. The geometry of the oil film and the pad has a significant influence on the operating characteristics of the plain thrust bearing. Hence, it is necessary to take into account in the tests of these bearings the changes in the geometry of the oil film that result from the variations of forces acting on the bearing pad under various operating conditions.
4. Load capacity and friction torque as well as the maximum oil film pressure and temperatures vary linearly in the range of rotational speeds from 50 rpm up 800 rpm; over the highest assumed speed there is also linear but higher increase in all of these parameters.
5. The adiabatic model of flow assures the sufficient accuracy in the calculation of thrust axial bearings. The differences in the values of the calculated parameters that characterize the operation of the bearing are negligible between the adiabatic and diathermic models. However, the diathermic model of oil film should be considered while taking taken into the thermoelastic deformations of tilting pads.

REFERENCES

1. Idzikowski M.: Effect of the surface macrogeometry on the operation of axial thrust bearing. Ph. D. Thesis. Lodz University of Technology. Łódź. 1976.(in Polish).
2. Kusmierz L.: Analysis of elastic deformations of tilting pads on the operating characteristics of axial thrust bearing. Ph. D Thesis. Lodz University of Technology. Łódź. 1980. (in Polish).
3. Murdzia E.: Thermohydrodynamic characteristics of thrust bearing. Ph. D. Thesis. Lodz University of Technology. Lodz. 1980 (in Polish).
4. Wasilczuk M.: Large overall dimensions axial thrust bearings. Radom: Scientific Publisher House of the Institute of Technology and Exploitation. 2012 (in Polish).
5. Rathish Kumar R.B., Yamaguchi T.Y., Himeno R.A.: THD Analysis of High-Speed Slider Bearing with Injection. Synopses of the International Tribology Conference Nagasaki, 2000. 3P1-7.
6. Glavatski S.B., Fillon M.: TEHD Analysis of Tilting-Pad Thrust Bearings – Comparison with Experimental Data. Synopses of the International Tribology Conference Nagasaki, 2000. 4E1-1.
7. Murdzia E., Strzelecki S.: Computer program of the computation of tilting-pad thrust bearings. 2020.
8. Fillon M., Wodtke M., Wasilczuk M.: Effect of presence of lifting pocket on the THD performance of a large tilting-pad thrust bearing. *Journal of Friction and Wear*, 3(4), 2015, pp. 266–274.
9. Wodtke M., Schubert A., Fillon M., Wasilczuk M., Pajęczkowski P.: Large hydrodynamic thrust bearing: Comparison of the calculations and measurements. *PROCEEDINGS OF THE INSTITUTION OF MECHANICAL ENGINEERS PART J-JOURNAL OF ENGINEERING TRIBOLOGY*, 228, 2014. 974-983. <https://doi.org/10.1177/1350650114528317>.
10. Wasilczuk M., Wodtke M., Dąbrowski L.: Field Tests on Hydrodynamic and Hybrid Operation of a Bidirectional Thrust Bearing of a Pump-Turbine. *Lubricants*, Vol. 5, 2017, nr. 4, pp. 1–13.
11. Wodtke M., Fillon M., Schubert A., Wasilczuk M.: Study of the Influence of Heat Convection Coefficient on Predicted Performance of a Large Tilting-Pad Thrust Bearing. *JOURNAL OF TRIBOLOGY-TRANSACTIONS OF THE ASME*. -Vol. 135, 2013, Iss. 2, pp. 1–11.
12. Fillon M., Wodtke M., Wasilczuk M.: Effect of presence of lifting pocket on the THD performance of a large tilting-pad thrust bearing. *Journal of Friction and Wear*. -Vol. 3, 2015. Iss. 4, , pp. 266–274.
13. Chmielowiec-Jablczyk M., Schubert A., Kraft C., Schwarze H., Wodtke M., Wasilczuk M.: Improvement of the thrust bearing calculation considering the convective heating within the space between the pads. 16th EDF/Pprime Workshop: Behaviour of journal and thrust bearings under transient and mixed lubrication regime. 2017, pp. 1–12.
14. Rotta G., Wasilczuk M.: Modeling lubricant flow between thrust-bearing pads. *TRIBOLOGY INTERNATIONAL*. Vol. 41, 2008. Iss. 9-10, , pp. 908–913.
15. Bouyer J., Wodtke M., Fillon M.: Experimental research on a hydrodynamic thrust bearing with hydrostatic lift pockets: Influence of lubrication modes on bearing performance. *TRIBOLOGY INTERNATIONAL*. Vol. 165, 2022. Article 107253.